Towards Reliable Crack Growth Monitoring: A Preliminary Study on Fiducial Marker-Based Camera Repositioning Errors

JIRI KUNECKY

ABSTRACT

This study explores the precision and practical feasibility of using fiducial markers and projective transformations for non-contact displacement measurement in structural monitoring applications. By tracking a grid of ArUco markers affixed to a planar surface, image alignment was achieved using homography-based rectification, enabling subpixel accuracy in displacement and strain evaluation. A high-resolution industrial camera setup with calibrated optics and image averaging was used to minimize noise. The impact of camera repositioning errors - translational and rotational – on displacement accuracy was systematically evaluated through three controlled scenarios. Results show that while minor displacements (e.g., 5 mm shifts) can introduce errors up to hundreds of micrometres, careful alignment and the use of projective correction significantly reduce this effect. The findings highlight both the promise and the limitations of this low-cost, repeatable approach, especially for applications such as crack monitoring, where high spatial precision is required.

Jiří Kunecký, Institute of Theoretical and Applied Mechanics of the Academy of Sciences of the Czech Republic, Prosecká 811/76, Prague, Czech Republic. email: kunecky@itam.cas.cz.

INTRODUCTION

Monitoring rigid body motion or crack length over time can be challenging due to various factors, including the high cost, the risk of equipment damage or theft, and the need for advanced technology on-site. Non-contact technologies, such as marker-based evaluation of image sequences, offer a promising solution. However, to ensure accurate tracking, images must be captured from the same position over time, necessitating the use of fixed reference points. Ideally, these reference points should remain stationary, but in practice, they may shift. Therefore, the most effective approach is to attach a set of markers to the 2D planar object and treat a subset of these markers as rigid, assuming minimal deformation.

The repositioning process is subject to several sources of error, including environmental factors (moisture, temperature), camera calibration inaccuracies, algorithmic issues, and noise. Despite these challenges, when dealing with 2D planar strains, the validity of projective transformation can be relied upon. This transformation requires a pair of four points in the image to represent the state before and after deformation. Fiducial markers (for more see [1] and [2]), commonly used in computer vision, are ideal for this purpose as they allow precise positioning and incorporate an ID encoded in the marker's binary code. Such a method is commonly known and well implemented, a few papers have been published to date, e.g. [3].

By applying projective transformation [4], one can align the image to its original state. The transformed image can then be analysed using computer vision algorithms, such as digital image correlation, or by tracking the fiducial markers directly (as we show here). This approach is cost-effective, fast, repeatable, and sufficiently accurate for many applications. This study presents an experiment to evaluate the precision of this technique in a real-world setting, especially to quantify the error in order to assess if the method is suitable for a given task.

METHODS

The experimental setup employed a Basler a2A5320-7gmPRO industrial camera, offering high-resolution image (set as square 3040x3040 px) capture suitable for precise feature localization. The camera was equipped with a Fujinon CF25ZA-1S lens (23 MP, 25 mm focal length), selected for its low distortion and compatibility with the sensor resolution. To ensure accurate intrinsic calibration, a 9×6 chessboard pattern was used. The calibration process followed standard OpenCV routines, resulting in estimation of the camera matrix and radial and tangential distortion coefficients. The camera was mounted on a Manfrotto tripod equipped with two Manfrotto slides screwed together at 90° - including millimetre scales, providing stable and repeatable positioning during image acquisition. For marker and target printing, a standard office OKI C833 laser printer with 1200 DPI resolution was used.

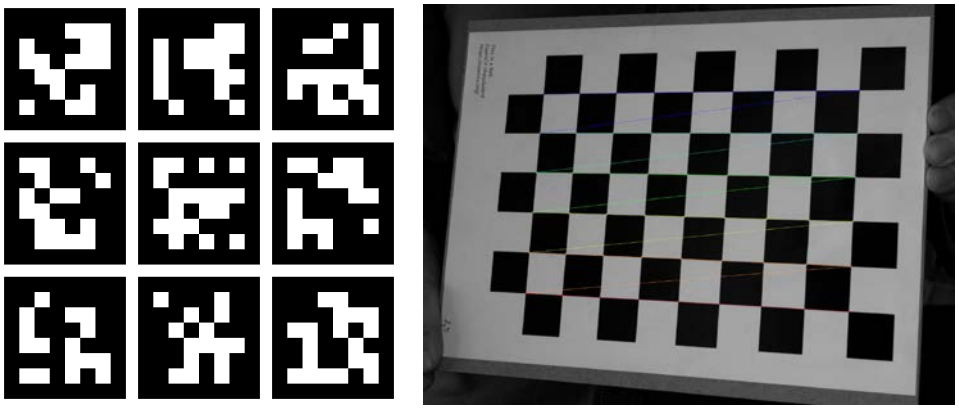

Figure 1. ArUco fiducial markers (left) and the chessboard used for calibration of the camera (right)

A 3×3 grid of fiducial markers (see Fig. 2) was prepared using the ArUco dictionary 6x6_250. Each marker was rendered at a resolution of 400×400 pixels, corresponding to a physical size of 40 mm, resulting in a print resolution of 10 pixels per millimetre. Markers were printed on vinyl paper to avoid influences of environmental changes, and matte finish ensured reflectless marker detection. The marker grid was mounted on a vertical interior wall using office glue, allowing for secure and relatively flat placement. A standard laser level was used during installation to align the markers as accurately as possible. The distance between neighbouring marker centres was set to 320 mm, creating a regular grid layout for spatial referencing. During image acquisition, the camera was positioned approximately 2700 mm from the wall, oriented perpendicular to the surface and centred on the middle marker in the grid. This setup provided a clear field of view covering the entire marker grid with sufficient resolution for pose estimation and subsequent analysis. For measurement of rotation in the tripod plane in the XZ-axis (see Fig. 2) a standard laser meter was used and the distances measured using trigonometry.

Figure 2. Camera setup with visible grid of ArUco markers (left), coordinate system of camera (right)

Image acquisition was performed using Pylon 6 software. To reduce random image noise and improve the accuracy of marker detection, each final image was obtained by averaging 100 consecutive frames. This approach effectively smoothed out sensor noise while preserving the sharp features of the markers. The entire processing pipeline – including marker detection, image warping and data analysis – was implemented in Python using NumPy [5], SciPy [6], and OpenCV 4.10 [7]. These tools enabled efficient numerical operations, image filtering, and robust application of computer vision algorithms throughout the workflow.

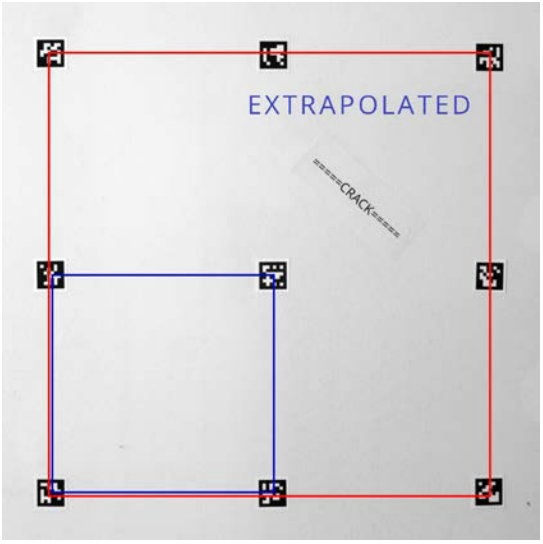

Figure 3. The two groups of results shown in the paper, red (bigger) square represents simple rectification to the whole area, blue (smaller) square represents rectification/realignment of just a subset of the original canvas, the area outside the blue rectangle is extrapolated/warped using homography from the four selected markers.

Fig. 3 illustrates the core concept of the experiment. The scene shown there served as a canvas to demonstrate the main idea. Since the markers remained fixed throughout the procedure, any observed discrepancy between images can be attributed solely to camera repositioning error - along with additional sources of error discussed later in the Results and discussion section.

At one point in time, a reference image was acquired by averaging 100 frames. Then, the camera was deliberately repositioned, and a second image was taken. In both images, four corresponding points - defined by specific marker IDs - were located with subpixel precision using corner refinement (MaxIterations=1e3, MinAccuracy=1e-3). Because the four markers lie in a single plane, a homography could be computed to relate the two images (projective transformation is valid!). The newly captured image was then warped to align with the reference image using this homography. To sum it up, the results do not show the strain caused by change of camera position, but the difference of rectified image aligned to the reference one and the difference is again found.

In the case of the red square, displacement vectors across the interior region were interpolated using radial basis functions (RBFs), and von Mises strain was calculated following standard methods from solid mechanics. The red square

simulates a situation, when the crack is just a singularity but the whole structure does not deform.

The blue square illustrates a different point: it shows how unreliable the alignment can become if only part of the marker field is used for registration and the remainder is extrapolated. This is particularly relevant for practical applications where a crack or defect might appear in the extrapolated area - beyond the region of accurate alignment. The results highlight the magnitude of error that can be introduced during camera repositioning and help define the acceptable tolerance for such repositioning in monitoring scenarios.

To evaluate the magnitude and nature of errors introduced by camera displacement, we defined three representative repositioning scenarios: (i) a 5 mm translation of the camera in the X direction, (ii) a 5 mm backward shift along the Z axis (increasing the distance from the object), and (iii) a 1-degree rotation in the XZ plane. These values were selected to reflect realistic positioning variations that may occur during manual camera repositioning without specialized equipment. The results for each scenario are presented using the same structure and logic to facilitate direct comparison.

RESULTS AND DISCUSSION

The measured and computed values are summarized in Tab. 1. The noise level indicates the resolution of the measurement method when the camera remains stationary. While this is specific to the demonstrated camera setup, similar issues are commonly encountered in practice. The measurement error (e.g., approximately 20 μm across the entire ‘red’ field) can be significantly reduced if the object is closer, the marker size is larger, or image averaging is performed over more frames. However, due to the many degrees of freedom involved, it is difficult to fully quantify the output within the scope of this brief conference proceedings paper.

Focusing on the alignment of the ‘blue’ square reveals a consistent trend: extrapolated values become significantly less precise in all cases. When the camera is repositioned with an error of 5 mm, the resulting measured displacements can range from around 100 microns to as much as 300 microns, but they never reach as much as 1 millimetre. With sensitive equipment and camera position correction methods - such as OpenCV solvePnP algorithm [7] using a predefined marker grid - the repositioning error can be reduced to around 1–2 mm, which substantially lowers displacement measurement error. This is promising for displacement monitoring applications, particularly for crack detection, where tell-tales often provide even lower resolution.

Interestingly, a 5 mm displacement of the camera along the Z-axis has little effect on measurement precision. This is likely due to the absence of perspective distortion and results that are comparable to the noise-only values. Again, the blue-field results show significantly greater scatter in displacement measurements. The largest and most detrimental reprojection error occurs in cases of rotational misalignment, which should therefore be strictly avoided during camera repositioning.

All results are also presented as contour plots in Fig. 4. These clearly show that noise remains a significant factor, and that the size of the reference points plays a crucial role in achieving precise measurements. The author believes these measurement errors can be further reduced by employing more sophisticated

methods, provided that repeated, quantified measurements of crack sizes can be obtained and the marker scale is visible in the images.

TABLE I. RESULTS - RANGE OF VALUES showing the amount of error

CAMERA REPOSITIONING ERROR	CASE	ΔUX [μm]	ΔUY [μm]	Δε []
Noise only	BIG SQUARE	18.0	5.3	1.62e-5
	SMALL SQUARE	64.8	24.3	3.24e-5
5 mm X	BIG SQUARE	108.0	45	9e-5
	SMALL SQUARE	360.0	360.0	20e-5
5 mm Z	BIG SQUARE	16.2	16.2	1.6e-5
	SMALL SQUARE	80.0	54.0	5.4e-5
1° rot XZ	BIG SQUARE	405.0	160	36e-5
	SMALL SQUARE	1215	1320	81e-5

CONCLUSIONS

A limited sample of displacement error analysis resulting from camera movement in various directions is presented in this work. The results demonstrate that tracking fiducial markers - originally developed for rapid orientation of robotic cameras - can offer a low-cost and straightforward method for measuring displacements on the order of tens of micrometres. When the camera is repositioned, it must be done with high precision; however, the projective transformation method used here achieves nearly two orders of magnitude better accuracy than the actual repositioning error. For example, a 5 mm displacement of the camera along the Z-axis would typically correspond to a strain field of $5/2700 \approx 1.8\times10^{-3}$, whereas the method presented here yields a strain of approximately 1.6×10^{-5}.

It is highly complex to account for all potential influences - such as distortion effects, camera intrinsics, depth of field, and others - which is why the authors focused on a representative dataset to illustrate the potential applicability of this method. Future work will aim to improve camera realignment accuracy through the use of a motorized positioning platform.

ACKNOWLEDGEMENT

The research was co-funded by the European Union under the project INODIN, no. CZ.02.01.01/00/23_020/0008487.

	ALIGNED BIG SQUARE	ALIGNED SMALL SQUARE
Noise only	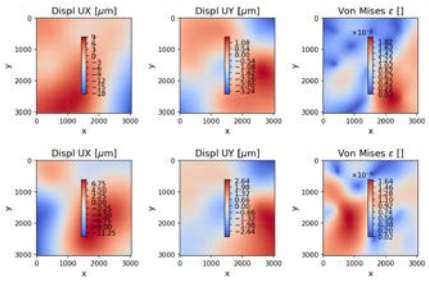	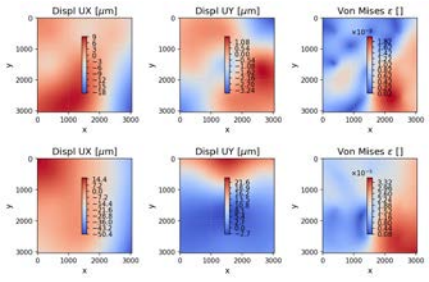
5 mm X	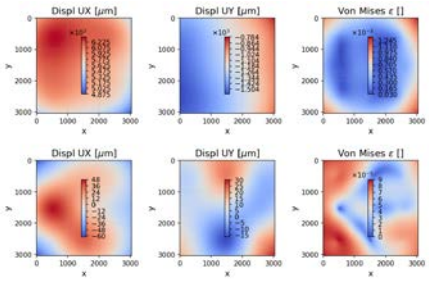	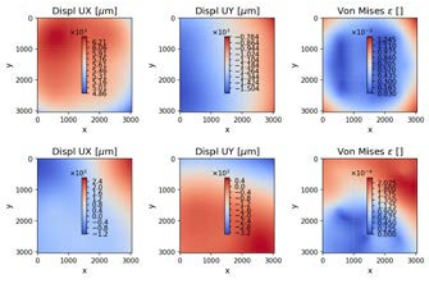
5 mm Z	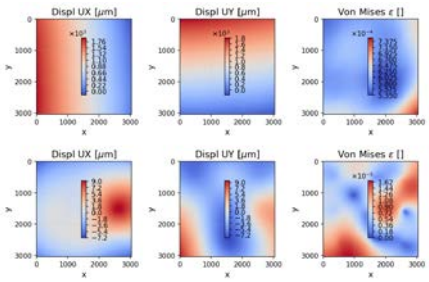	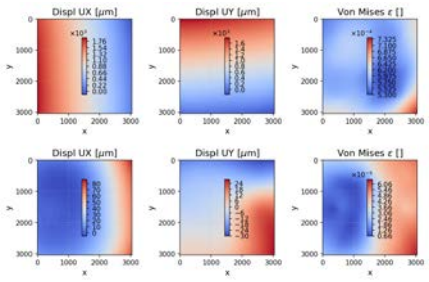
1° rot XZ	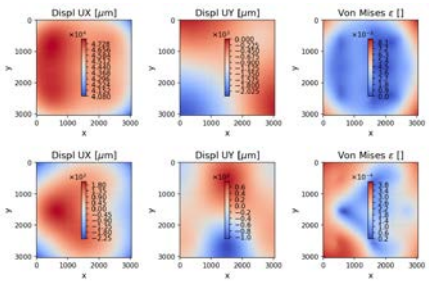	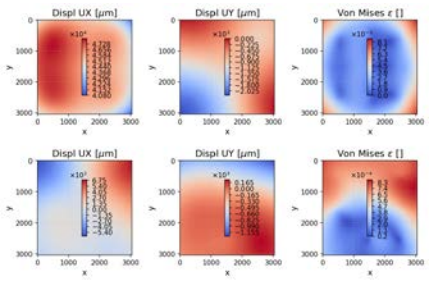

Figure 4. Results of the analysis expressed as contour plots

REFERENCES

1. Romero-Ramirez, Francisco J., Rafael Muñoz-Salinas, and Rafael Medina-Carnicer. 2018. “Speeded Up Detection of Squared Fiducial Markers.” *Image and Vision Computing* 76: 38–47.

2. Garrido-Jurado, S., R. Muñoz-Salinas, F. J. Madrid-Cuevas, and R. Medina-Carnicer. 2016. “Generation of Fiducial Marker Dictionaries Using Mixed Integer Linear Programming.” *Pattern Recognition* 51: 481–491.

3. Bontemps, A., Godi, G., Fournely, E. *et al.* Implementation of an Optical Measurement Method for Monitoring Mechanical Behaviour. *Exp Tech* **48**, 115–128 (2024). https://doi.org/10.1007/s40799-023-00636-2

4. Beardsley, P. “Projective Transformations.” Accessed February 14, 2025. https://homepages.inf.ed.ac.uk/rbf/CVonline/LOCAL_COPIES/BEARDSLEY/node3.html.

5. Harris, C.R., Millman, K.J., van der Walt, S.J. et al. *Array programming with NumPy*. Nature 585, 357–362 (2020). DOI: 10.1038/s41586-020-2649-2.

6. Pauli Virtanen, Ralf Gommers, Travis E. Oliphant, Matt Haberland, Tyler Reddy, David Cournapeau, Evgeni Burovski, Pearu Peterson, Warren Weckesser, Jonathan Bright, Stéfan J. van der Walt, Matthew Brett, Joshua Wilson, K. Jarrod Millman, Nikolay Mayorov, Andrew R. J. Nelson, Eric Jones, Robert Kern, Eric Larson, CJ Carey, İlhan Polat, Yu Feng, Eric W. Moore, Jake VanderPlas, Denis Laxalde, Josef Perktold, Robert Cimrman, Ian Henriksen, E.A. Quintero, Charles R Harris, Anne M. Archibald, Antônio H. Ribeiro, Fabian Pedregosa, Paul van Mulbregt, and SciPy 1.0 Contributors. (2020) **SciPy 1.0: Fundamental Algorithms for Scientific Computing in Python**. *Nature Methods*, 17(3), 261-272. DOI: 10.1038/s41592-019-0686-2.

7. Bradski, Gary. 2000. “The OpenCV Library.” *Dr. Dobb's Journal of Software Tools*.